Microstructure and Hardness Distribution of Friction Stir Welded 1050 Al and IF Steel with Different Original Grain Sizes†

SUN Yufeng *, FUJII Hidetoshi **, TAKADA Yutaka *, TSUJI Nobuhiro **, NAKATA Kazuhiro **, NOGI Kiyoshi ****

Abstract

In this study, 2mm-thick commercial 1050-Al plates and IF steel plates with three different kinds of original grain size were subjected to the friction stir welding process. These three kinds of samples with different grain sizes were obtained by accumulative roll bonding after a 5 cycles process, 5 cycles ARB process plus annealing and fully annealing, respectively. The microstructure evolution and Vickers hardness in the stir zone of all the samples were investigated. For both 1050-Al and IF steel, the ARB plus annealed samples with an intermediate original grain size finally produced the most refined microstructure and highest Vickers hardness in the stir zone. While for the ARB processed samples with ultrafine grained structure, significant grain growth and decrease in hardness occurred in the stir zone. The microstructure coarsening in the stir zone is suggested to be caused by the heating of the unstable structure in the ultrafine grained materials during friction stir welding process.

KEY WORDS: (Friction stir welding) (Accumulative roll bonding) (Ultrafine grained structure) (Vickers hardness)

1. Introduction

Recently, ultrafine grained (UFG) materials have attracted growing interest among material scientists due to the rapid development of severe plastic deformation (SPD) technique like accumulative roll bonding (ARB), equal channel angular pressing (ECAP) and high pressure torsion (HPT). The UFGed materials have an average grain size of less than 1 μm and usually exhibit superior mechanical properties to their coarse grained counterparts [1-5]. For example, 6 cycle ARB processed pure aluminum shows a high strength compared to that of low carbon steel [6]. Nowadays, UFGed materials can be produced in bulk size through several SPD methods. However, because of some limitations of these SPD techniques such as the load capacity and rigidity of the equipment, the UFGed materials still cannot be made large enough for extended industrial applications. Therefore, the welding or joining of UFGed materials to produce a larger size should be reconsidered. Obviously, the UFGed materials can not be welded by the commonly used fusion process, because the molten pool generated during welding will inevitably destroy the ultrafine structure and result in much coarser grains in the solidified joint. Comparatively, friction stir welding (FSW) seems to be a very promising approach to solve the welding problems of the UFGed materials up to the present day.

FSW technique is regarded as a relatively new solid-state welding process, which was invented by TWI in 1991 with an attempt to weld aluminum alloys [7]. Compared with other welding techniques, FSW is much more energy efficient, environment friendly and versatile. Up to now, many kinds of aluminum alloys from commercial pure aluminum to highly alloyed 2XXX and 7XXX series, which are generally considered as non-weldable, have been successfully joined by FSW technique. Nowadays, the application of FSW has been widely extended to a variety of materials including steel, copper, titanium alloys and even polymers [8-10]. However, because most FSW processed materials are conventional metals with grain size larger than 1 μm, not much attention has been paid to the effects of grain size on the joint properties. Since the heat generated by the friction from the rotation tools will inevitably lead to a temperature rise, it might bring the risk of

† Received on December 18, 2009
* Specially Appointed Researcher
** Professor
*** Graduate Student

Transactions of JWRI is published by Joining and Welding Research Institute, Osaka University, Ibaraki, Osaka 567-0047, Japan

recrystallization and coarsening of the UGFed materials. Therefore, the size effect plays an important role in the joint properties of the UFGed materials being welded. Previously, Sato and Topic et al. compared the hardness distribution in the stir zone of the ECAP and ARB processed aluminum with their coarse counterparts and found that hardness decrease did take place in the FSW processed materials with the UFGed structure due to the coarsening of grain size [11-14]. Fujii et al. also observed the same phenomena in the ARB processed IF steel [15, 16].

In this study, 2 mm-thick commercial 1050-Al plates and IF steel plates with an UFGed structure were obtained after a 5 cycle ARB process. The ARB processed plates were then FSW processed at various revolution pitches (welding speed/ rotation speed). For comparison, as-received materials with coarse grains and ARB plus annealed samples with an intermediate grain size were also FSW processed under the same conditions. The microstructure evolution and mechanical properties of these three kinds of samples with different initial grain sizes after the FSW process were investigated and the mechanism of the initial grain size dominated welding properties is discussed.

2. Experimental

In this study, the as-received commercial purity 1050-Al plates and ultra low carbon IF steel in the fully annealed state were used as the starting materials. To obtain different grain sizes in the workpiece being welded, the as-received plates were first subjected to 5 cycles ARB process. As a result, the ARB processed materials have an UFGed microstructure with average grain size less then 1μm. In order to obtain a sufficient bonding strength, the IF steel plates were heated in a furnace at 500℃ for 10 min before each ARB cycle. After the roll bonding, the samples were cooled immediately in water. The details of the ARB process are described in refs [17, 18]. Next, some of the ARB processed Al plates were annealed under the H24 condition to obtain partially grown grains. While for IF steel, the plates were annealed at 600℃ for 1.8 ks. However, the grain size of the annealed samples is still much less than that of the as-received sample. These three kinds of materials with different initial grain sizes, that is, the as-ARBed samples, the ARB + annealed samples, together with the as-received samples, were then butt-welded along the rolling direction (RD) using an FSW machine. The samples used in the FSW process were 2 mm thick plates of 300 mm in length and 30 mm in width. In every FSW batch, two sample plates were put together and then FSW processed parallel with the rolling direction. During the welding process, the rotation tool was titled by 3°, and had a 12 mm-dia shoulder, 4 mm-dia probe and 1.8 mm probe height. For the FSW of Al, a travel speed of 1000 mm/min and rotation speed of 600 rpm were used, which corresponds to a revolution pitch of 1.67 mm/r. While for the FSW of IF steel, a travel speed of 400 mm/min and rotation speed of 400 rpm were used, which corresponds to a revolution pitch of 1 mm/r. The revolution pitch is smaller for the welding of IF steel due to its relatively higher melting temperature and higher strength so that more heat input is necessary to obtain a sound weld. During the entire welding process, the temperature variations at the center of the welds were monitored using a thermocouple fixed at the bottom surface of the workpieces.

For both Al and IF steel welded samples, the Vickers hardness was measured on the centerline of the cross-section perpendicular to the welding direction. The microstructures of the welded samples were characterized by optical microscopy, transmission electron microscopy (TEM) and the electron back-scattering diffraction (EBSD) technique. Thin foils perpendicular to the transverse direction (TD) and parallel to the welding direction were cut from the center of the weld for TEM observations and the planes parallel to the TD were cut from the weld for EBSD measurements. The cut specimens were then twin-jet electropolished in a mixed solution of HNO_3:CH_3OH=3:7 for Al and HCO_4:CH_3COOH=1:9 for IF steel. The EBSD measurements were carried out using a program developed by TSL (OIM-Analysis 3.0x) in a Philips XL30 SEM equipped with a field emission (FE) gun operated at 15 kV. The TEM observations were performed using a Hitachi H800 TEM operated at 200 kV.

3. Results and Discussion

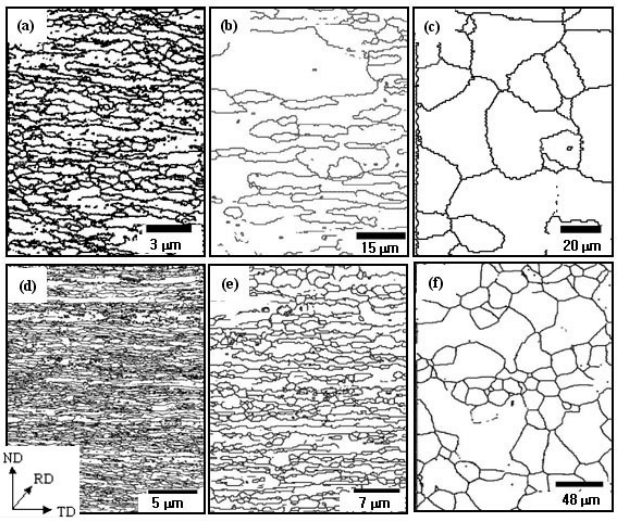

Fig. 1 Grain boundary maps of 1050-Al and IF steel with different grain size. (a) ARB processed Al; (b) ARB+annealed Al; (c) as-received Al; (d) ARB processed IF steel; (e) ARB+annealed IF steel and (f) as-received IF steel.

Figure 1 shows the typical grain boundary maps of the starting materials for the FSW process that were obtained from the EBSD measurements. The grain size and morphology of the ARB processed Al, ARB + annealed

Al and the as-received Al are shown in **Fig. 1(a)**, **1(b)** and **1(c)**, respectively. While the grain size and morphology of the ARB processed IF steel, ARB + annealed IF steel and the as-received IF steel are shown in **Fig. 1(d), 1(e)** and **1(f)**, respectively. All the maps were observed from the TD. In these maps, only high angle boundaries with misorientations higher than 15° are indicated by black lines. In general, the Al and IF steel show the same trend of microstructure evolution after different treatment, i.e., ARB processing and ARB+annealing treatment. It can be seen that after different treatments both Al and IF steel exhibit quite different microstructures and different mean grain sizes compared with their as-received counterpart. The as-received samples have a fully annealed feature of very coarse equiaxial grains. While the ARB processed sample showed an ultrafine lamellar structure with the mean boundary interval less than 1 μm. Significantly elongated grains with lengths ranging of several micrometers were observed parallel to the TD. However, for the ARB+annealed samples, heat induced grain growth can be easily found and the originally elongated grains become larger and somewhat equiaxial. But the lamellar structure remained somewhere with a thicker boundary interval. In addition, the mean grain sizes of both the annealed samples lie between that of the as-received samples and the as-ARB processed sample.

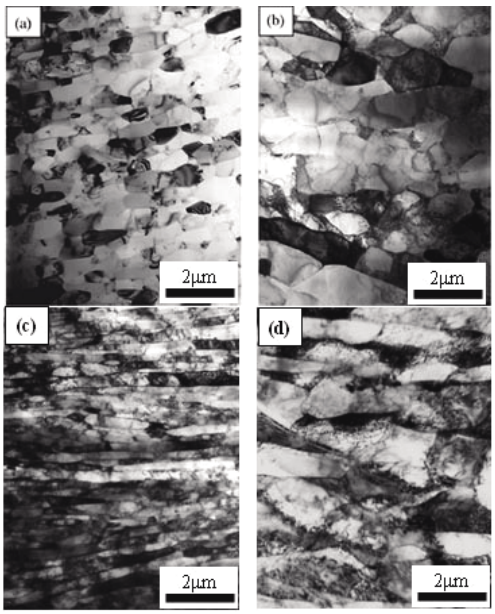

Fig. 2 TEM images showing the microstructure of (a) ARB processed Al; (b) ARB + annealed 1050 Al; (c) ARB processed IF steel and (d) ARB + annealed IF steel.

The detailed microstructures of the treated Al and IF steel were studied by TEM observations. **Figure 2 (a)** and (b) show the typical TEM images of the ARB processed and ARB+annealed Al samples. While **Fig. 2(c)** and **(d)** show the typical TEM images of the ARB processed and ARB+annealed IF steel samples. It is not easy to obtain the global microstructure of the as-received sample under TEM observation, since the grain size is too big. For the as-ARB processed samples shown in **Fig. 2 (a)** for Al and **Fig. 2(c)** for IF steel, the lamellar boundaries are quite straight along the rolling direction. The microstructure in the ARB processed sample showed rather pancake-shaped ultrafine grains nearly free from dislocations inside presumably due to the recovery and short range of gain boundary migration. The lamellar structure is uniform throughout the entire sample and the mean interval of the lamellar boundary is about 600 nm for Al and 400 nm for IF steel. However, for the annealed samples shown in **Fig.2 (b)** for Al and **Fig. 2(d)** for IF steel, the pancake-shaped ultrafine grained structure can hardly be discerned and most of the grains are equiaxial, with a grain size larger than that of the as-ARBed samples. Some dislocation can still be found inside some grains or aggregates at some of the grain boundaries.

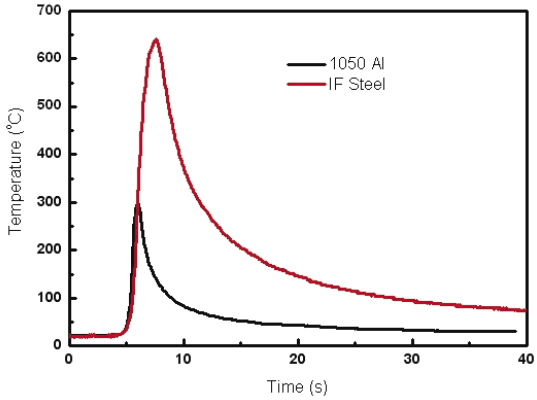

Fig. 3 Thermal profiles measured at the back of workpieces during FSW process.

For both Al and IF steel, the as-received plates as well as those after ARB and ARB+annealing treatment were then applied to the FSW process. The thermal profiles were measured at the back of the workpieces during the FSW process. It was found that the thermal profiles are identical for the FSW of same materials, despite of the variation in original grain size. **Figure 3** shows the thermal profile of Al and IF steel during the welding process. For both Al and IF steel, the temperature rises sharply to its maximum value when the rotating tools passed through the locations where the thermocouples were fixed in the workpiece. The temperature peaks during FSW of Al is about 300℃. While the temperature peak during the FSW of IF steel is about 640℃, which is much lower than the α/γ transformation temperature (910℃). Considering that the melting points of pure Al and IF steel are 660℃ and 1530℃ respectively, the temperature ratio T_r/T_m of the maximum temperature rise (T_r) to the melting point (T_m) is about 0.614 for Al and 0.506 for IF steel. When the rotation tool passed by, the temperature then decreased gradually down to room temperature. However, it takes

much longer period for the IF steel than Al to cool down from the maximum temperature to the room temperature. It was suggested that the smaller revolution pitch for the FSW of IF steel caused the higher temperature rise, however, the lower thermal conductivity of IF steel explains the longer time cooling after welding.

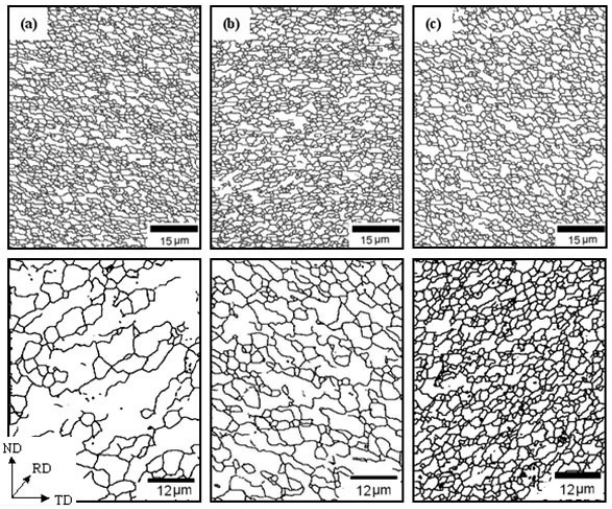

Fig. 4 Grain boundary maps in the stir zone of the FSW processed samples. (Observed from TD). (a) as-received Al; (b) ARB processed Al; (c) ARB +annealed Al; (d) as-received IF steel; (e) ARB processed IF steel and (f) ARB +annealed IF steel.

After FSW process, the microstructures at the geometric center of the stir zone were characterized by EBSD measurements. As a typical example, **Figure 4** shows the grain boundary maps of both the Al and IF steel samples. **Figure 4 (a), (b)** and **(c)** show the size and morphology of grains in the stir zone of ARB processed, ARB+annealed and as-received Al, respectively. While **Fig. 4 (e), (f)** and **(g)** show the size and morphology of grains in the stir zone of ARB processed, ARB+annealed and as-received IF steel, respectively. In all the maps, the black lines in the figure separated the grains with grain boundary misorientations larger than 15°. For both Al and IF welds, only equiaxial grains can be found in the grain boundary maps and the elongated grains in the ARB processed or the ARB + annealed samples cannot be found any more. For either Al or IF steel weld, the ARB + annealed sample exhibits the smallest grain size, although its original grain size falls between that of the as-received and as-ARBed counterparts. It is worth mentioning that the grain size increases after the FSW process in the as-ARB processed sample. This phenomenon is quite unique since the usually refined structure can be obtained in the stir zone due to dynamic recrystallization. The average sizes of the grains with a high-angle boundary obtained from the EBSD measurements of all the samples were summarized in Table 1.

Figure 5(a), (b) and **(c)** show the typical TEM bright field images of the stir zones in the as-received, ARB processed and ARB + annealed Al respectively. While **Fig. 5(d), (e)** and **(f)** show the typical TEM bright field images of the stir zones in the as-received, ARB processed and ARB + annealed IF steel respectively. For both Al and IF steel, the microstructure evolution after FSW process exhibits a very similar trend. For example, in ARB processed Al and IF steel, no pancake structure can be observed after FSW process. In addition, the microstructure characterization reveals that all the samples consist of equiaxial grains with dislocations inside and the dislocation densities were not very high after severe plastic deformation induced by the FSW. However, the dislocation density in the stir zone of IF steel seems to be higher than that in the stir zone of pure Al, which is one of the specific materials that are easy to recovery due to its high stacking fault energy. Another reason probably is related to the restricted recovery of IF steel during the FSW process because of the lower temperature ratio T_r/T_m comparing with that of Al. In addition, from the TEM observations, we found that after the FSW process the grain size in the stir zone of the previously annealed sample was the smallest among the three kinds of samples, which agrees well with the EBSD measurements.

Table 1. Grain size of the base materials and the stir zone of 1050 Al and IF steel (μm).

Samples	Base material (μm)		Stir zone (μm)	
	1050 Al	IF steel	1050 Al	IF steel
As-received	13.1	24.2	1.8	2.4
ARB+Annealed	8.4	1.8	1.6	0.9
ARBed	0.6	0.7	1.7	1.1

As is well known, the evolution of the grain structure in the stir zone during the FSW may depend on the grain boundary structure, grain size and dislocation density of the initial microstructure. Usually, when the FSW technique is applied to conventional metals or alloys, the grain structure in the stir zone is formed by dynamic recrystallization, which is characterized by a strain-induced progressive rotation of the subgrains with little boundary migration during the FSW process [12]. This process will eventually result in a significantly grain refinement and correspondingly higher strength in the stir zone than in the base material. However, when ultrafine grained materials like the ARB processed Al and IF steel in the present study were FSW welded, grain growth combined with a decrease in hardness were usually observed after the FSW process. Unlike conventional metals or alloys, a large quantity of vacancies or dislocations can be introduced into the ARB processed materials, which consist of pancake-shaped ultrafine grains mostly surrounded by high-angle boundaries. This kind of ultrafine grained microstructure was found to be quite unstable upon thermal treatment, although it exhibits quite high strength [19]. That is, recovery can

occur at relatively low temperatures to decrease the defect density within the grains. At the same time, continuous grain growth takes place and the mean grain size increases. At a lower temperature, the grain growth rate was relatively low and the grain boundary migration rate in both the direction parallel to the rolling direction and the direction perpendicular to the rolling direction were found to have a similar rate until the grains had reached equiaxial geometry. However, if the temperature is higher, for example, from 200 to 250℃ for commercial purity Al, the grain growth becomes very rapid. In this study, the temperature rise during the FSW of Al can reach 300℃ at the location where the rotating tools was passing through. Even at a revolution pitch of 2.5 mm/r, the temperature rise can reach above 250℃. Therefore, it was proposed that the fragmentation of the ultrafine grains by the shear stress during the FSW process is not significant, while the rapid grain growth in the unstable microstructure will eventually result in coarse grains. For the as-received and ARB + annealed samples, the microstructure is relatively stable and the grain subdivision during the FSW process dominates rather than the grain growth caused by the temperature rise. As a result, a grain refinement was finally obtained.

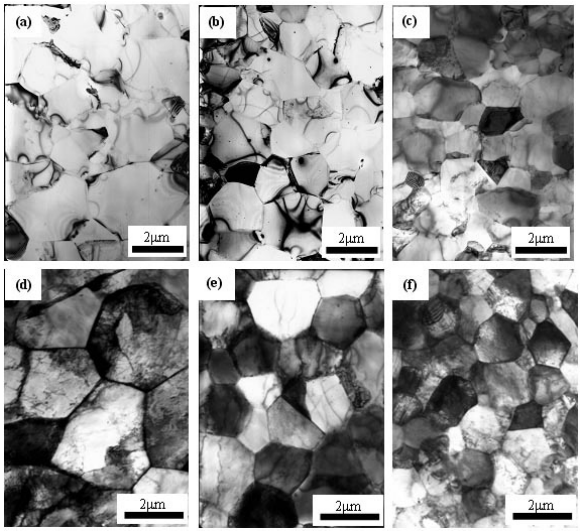

Fig. 5 TEM microstructures of stir zone of (a) as-received Al; (b) ARB processed Al; (c) ARB +annealed Al; (d) as-received IF steel; (e) ARB processed IF steel and (f) ARB +annealed IF steel.

Figure 6 shows the horizontal hardness profile measured from the transverse cross-section of 1050Al and IF steel welds with different original grain size. For both Al and IF steel, the hardness variations in the stir zone show the same trend. It can be seen that the as-received and ARB + annealed samples exhibit higher hardness in the stirred zone than in the base metals. While in the ARB processed sample, the FSW process resulted in an obvious reduction in hardness around the weld center. For example, the hardness of the ARB processed Al drops from 46 HV in the base metal to 31 HV in the stir zone. The ARB processed IF steel also shows the same phenomenon of hardness drop in the stir zone after FSW process. For all the samples, this hardness change spreads to about 5 mm away from the weld center on the centerline of the thickness of the plate, probably in the stir zone and TMAZ. Compared with the EBSD measurement, the Vickers hardness ordinarily increases with the decreasing grain size, which is generally in accordance with the classic Hall-Petch relationship.

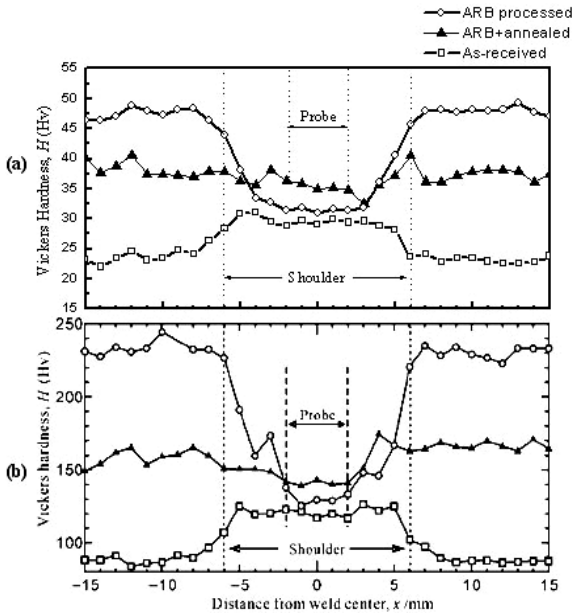

Fig. 6 Hardness profile of (a) Al and (b) IF steel joints.

4. Conclusions

In this paper, three kinds of 1050-Al alloy and IF steel plates with different original grain sizes, namely, an ultrafine grained structure obtained by the ARB technique, an intermediate grain size obtained by annealing the ARB processed sample, and the as-received materials with coarse grain structure in the fully annealed condition, were applied to the FSW process. The following conclusions can be drawn from the above experimental results.

a) The original grain size exerts a significant influence on the microstructure in the stir zone of both FSW processed 1050 Al and IF steel. The ARB plus annealed sample with the intermediate grain size is the most preferable for obtaining the highest hardness in the stir zone with the smallest grain size.
b) For both 1050 Al and IF steel, all the samples exhibit equiaxial grains in the stir zone despite of the initial grain shape or size of the materials. However, the dislocation density is a little higher in the stir zone of IF steel welds than that in the 1050 Al welds due to the lower temperature rise during the welding comparing with the high melting point of steel.

c) The ultrafine grained structure of the ARB processed sample is unstable. The grain growth in the stir zone is believed to be caused by the temperature rise during the FSW process.

Acknowledgements

The authors wish to acknowledge the financial support of a Grant-in-Aid for Science Research from the Japan Society for Promotion of Science and Technology of Japan, the Global COE Programs, a Grant-in-Aid for the Cooperative Research Project of Nationwide Joint-Use Research Institute from the Ministry of Education, Sports, Culture, Science and Toray Science Foundation, ISIJ Research Promotion Grant, and Iketani Foundation.

References

[1] R.Z. Valiev, R. K. Islamgaliev and I.V. Alexandrov. Prog in Mater Sci, 2000, 45, 103-189
[2] T.G. Langdon. Rev. Adv. Mater. Sci, 2006, 11, 34-40
[3] S. H. Lee, Y. Saito, N. Tsuji et al. Scripta. Mater, 2002, 46, 281-285
[4] N. Tsuji, Y. Saito, H. Utsunomiya, et al. Scripta.Mater, 1999, 40, 795-800
[5] N.Q. Chinh, P. Szommer, Z. Horita and T.G. Langdon. Adv. Mater, 2006, 18, 34-39
[6] N. Tsuji. J. Nanoscience and nanotechnology. 2007, 7, 3765-3770
[7] W. M. Thomas, E. D. Nicholas, J. C. Needham. Friction stir butt welding. International Patent Application No. PCT/GB92/02203; 1991
[8] L. Cui, H. Fujii, N. Tsuji and K. Nogi. Scripta Mater, 2007, 56, 637-640
[9] R. Nandan, T. Debroy and H.K.D.H. Bhadeshia: Prog in Mater Sci, 2008, 53, 980-1023
[10] Seth R. Strand. Effects of friction stir welding on polymer microstructure. Ph.D thesis, 2004, Brigham Young University.
[11] Y. S. Sato, M. Urata, H. Kokawa, K. Ikeda and M. Enomoto. Scripta.Mater, 2001, 45, 109-114
[12] Y. S. Sato, Y. Kurihara, S.H.C. Pack, H. Kokawa and N. Tsuji. Scripta. Mater, 2004, 50, 57-60
[13] I. Topic, H. W. Hoppel and M. Goken. Mater.Sci.Eng-A, 2009, 503, 163-166
[14] I. Topic, H.W. Hoppel and M. Goken. Mater.Sci.Forum, 2008, 584-586, part2, 833-839
[15] H. Fujii, R. Ueji, Y. Takada et al. Mater. Trans, 2006, 47, 239-242
[16] H. Fujii, Y. Takada, N. Tsuji and K. Nogi. Proceedings of IIW pre-Assembly meeting on FSW in Nagoya, 2004, 19-24
[17] Y. Saito, H. Utsunomiya, N. Tsuji and T. Sakai. Acta Mater, 1999, 47, 579-583
[18] N. Tsuji, Y. Saito, S.H. Lee and Y. Minamino. Adv. Eng. Mater, 2003, 5, 338-344
[19] Charles Kwan, Z. R. Wang. J. Mater. Sci, 2008, 43:5045-5051